

Neural and eye-specific defects associated with loss of the Imitation Switch (ISWI) chromatin remodeler in *Xenopus laevis*

Sara S. Dirscherl^a, Jonathan J. Henry^b, Jocelyn E. Krebs^{a,*}

^aDepartment of Biological Sciences, University of Alaska Anchorage, 3211 Providence Drive, Anchorage Alaska 99508

^bDepartment of Cell & Developmental Biology, University of Illinois, 601 S. Goodwin Ave., Urbana, IL 61801, USA

Received 10 November 2004; received in revised form 5 August 2005; accepted 5 August 2005

Available online 29 August 2005

Abstract

Imitation Switch (ISWI) is a member of the SWI2/SNF2 superfamily of ATP-dependent chromatin remodelers, which regulate transcription and maintain chromatin structure by mobilizing nucleosomes using the energy of ATP. Four distinct ISWI complexes have been identified in *Xenopus* oocytes. The developmental role of *Xenopus* ISWI, however, has not previously been investigated *in vivo*. Here we report the tissue specificity, developmental expression, and requirement of ISWI for development of *Xenopus* embryos. Whole mount *in situ* hybridization shows *ISWI* localized in the lateral sides of the neural plate, brain, eye, and in later stages, the spinal cord. Injection of antisense *ISWI* RNA, morpholino oligonucleotides or dominant-negative *ISWI* mutant mRNA into fertilized eggs inhibits gastrulation and neural fold closure. Genes involved in neural patterning and development, such as *BMP4* and *Sonic hedgehog* (*Shh*), are misregulated in the absence of functional ISWI, and ISWI binds to the *BMP4* gene *in vivo*. Developmental and transcriptional defects caused by dominant-negative *ISWI* are rescued by co-injection of wild-type *ISWI* mRNA. Inhibition of ISWI function results in aberrant eye development and the formation of cataracts. These data suggest a critical role for ISWI chromatin remodeling complexes in neural development, including eye differentiation, in the *Xenopus laevis* embryo.

© 2005 Elsevier Ireland Ltd. All rights reserved.

Keywords: ISWI; Chromatin remodeling; Development; SWI2/SNF2; Lens; Retina

1. Introduction

The embryonic development of multicellular organisms is a complex and orderly process that depends on precise regulation of spatial and temporal patterns of gene expression. Cell specification and differentiation require that some gene loci become constitutively or inducibly expressed, while other loci become actively silenced. Cell type-specific patterns of expression and repression must often be maintained through subsequent rounds of cell division to preserve cell-lineage fidelity. Transcription activation and repression occurs in the context of chromatin, a complex of DNA and proteins that compacts DNA into the eukaryotic nucleus. The repeating structural unit of chromatin is the nucleosome, which is composed of 147

base pairs of DNA wrapped around an octamer of histone proteins. The compaction of DNA into chromatin, which functions to keep the genome organized within the boundaries of the cell nucleus, also suppresses gene activity. An essential step in gene activation includes the remodeling of nucleosomes at target promoters and enhancers, which facilitates binding of transcription factors. A combination of chromatin remodeling enzymes and histone modifying enzymes establish a steady level of transcriptional control in all eukaryotes (Khorasanizadeh, 2004).

The ATP-dependent chromatin remodeling complexes use the energy of ATP hydrolysis to locally disrupt or alter the association of histones with DNA, or to slide nucleosomes along the DNA. ATP-dependent chromatin remodeling complexes can facilitate gene activation or repression by helping transcription factors or histone modifying enzymes gain access to their targets in chromatin. All of the ATP-dependent chromatin remodeling complexes contain a catalytic ATPase subunit that belongs

* Corresponding author. Tel.: +1 907 786 1556; fax: +1 907 786 1314.
E-mail address: afjek@uaa.alaska.edu (J.E. Krebs).

to the SWI2/SNF2 superfamily of proteins. These ATPases have been classified into several subfamilies, the largest of which are the SWI2/SNF2 group and the Imitation Switch (ISWI) group (Eisen et al., 1995).

Multiple ISWI-containing complexes have been identified in yeast, *Drosophila*, *Xenopus*, and mammals. ISWI complexes are involved in multiple nuclear functions, including transcriptional activation and repression, replication, and chromatin assembly (Dirscherl and Krebs, 2004). Null and dominant negative *ISWI* mutants have demonstrated that ISWI is essential for cell viability and required for gene expression during development in *Drosophila* (Deuring et al., 2000), including expression of homeotic genes (Badenhorst et al., 2002).

Homologs of *ISWI* have been identified in human and mouse (*Snf2 h* and *Snf2 l*) (Okabe et al., 1992; Aihara et al., 1998; Lazzaro and Picketts, 2001). Both *ISWI* homologs are expressed during development of the nervous system in mice, but they exhibit differential expression patterns (Lazzaro and Picketts, 2001). *Snf2 h* is transiently expressed in proliferating cell populations during embryogenesis and early postnatal development, while *Snf2 l* expression is upregulated in terminally differentiated neurons after birth and persists in adult animals. A human complex containing SNF2L is involved in the induction of neurite outgrowth in tissue culture (Barak et al., 2003). Intriguingly, the *Snf2 l* gene is localized to a region of the X chromosome associated with multiple X-linked mental retardation (XLMR) disorders (Lazzaro and Picketts, 2001).

Four ISWI-containing complexes have been identified in *Xenopus* through biochemical fractionation of *Xenopus* oocytes (Guschin et al., 2000), three of which are homologs of ISWI complexes in other species. The most abundant ISWI complex in oocytes is xACF (ATP-dependent chromatin assembly factor). *Xenopus* also contains CHRAC (chromatin accessibility complex) and WICH (WSTF-*ISWI* chromatin remodeling complex) (Bozhenok et al., 2002). The subunit composition of the fourth ISWI complex has not been elucidated. Comparison of the remodeling activity of *Xenopus* ISWI complexes in vitro fails to reveal significant qualitative or quantitative differences (Guschin et al., 2000). The subunits unique to each ISWI complex could determine the specific nuclear function for each complex (chromatin assembly vs. transcriptional regulation vs. replication). Unquestionably, the developmental program of *Xenopus*, with an early period of rapid nuclear divisions, places a special burden on the machinery for chromatin assembly and remodeling. The multiple ISWI complexes described here may reflect those specialized demands.

A number of SWI2/SNF2-family ATP-dependent chromatin remodelers have been linked to developmental processes. There are several developmental disorders in humans associated with loss of function of chromatin remodelers. These include: ATRX mutations and mental retardation (Picketts et al., 1996), SMARCAL1

and Schimke immuno-osseous dysplasia (Boerkoel et al., 2002), CSB and Cockayne syndrome (Citterio et al., 2000) and SNF2H and Williams syndrome (Bochar et al., 2000). Williams syndrome is a developmental disorder linked to the ISWI-containing complex WICH, which contains the Williams Syndrome Transcription Factor (WSTF) and therefore suggests a possible transcriptional role for this complex. WICH also appears to have a direct role in the replication of heterochromatin (Bozhenok et al., 2002).

We wish to understand the functional diversity of ISWI complexes by defining the functions of different ISWI complexes in the whole organism. We have begun by analyzing the role of the one subunit common to all the ISWI complexes, ISWI itself. In this study we use *Xenopus laevis* to examine the expression pattern and regulatory effects of *ISWI* in the developing vertebrate embryo. In situ hybridization reveals *ISWI* to be localized almost exclusively in neural tissue. We inhibited ISWI function in early embryos by three methods: microinjection of antisense mRNA or microinjection of morpholino oligonucleotides to inhibit the translation of endogenous *ISWI* mRNA, and microinjection of mRNA encoding a dominant negative mutant of *ISWI*. We have shown that ISWI knockdowns result in gastrulation defects, incomplete closure of the neural tube, delayed development, misexpression of neural-specific genes, eye malformations and the formation of cataracts. These results reveal an essential role for ISWI both in early development and in later stages of neural development.

2. Materials and methods

2.1. RNA for microinjection

A 3500 bp *ISWI* cDNA cloned into pBSKS was kindly provided by Dr Paul Wade (Emory University). This *ISWI* clone was digested with KpnI and PstI and a 343 bp fragment corresponding to nucleotides 2143–2486 was isolated and inserted into pBSSK to create a plasmid capable of transcribing an antisense RNA with the T3 promoter. Transcripts were synthesized using Megascript™ (Ambion, Austin, TX). For in situ hybridization the same procedure was used except a digoxigenin-labeled UTP was incorporated. A plasmid capable of transcribing a full length *GFP* mRNA was provided by Dr Richard Harland (UC Berkeley), and was used as an RNA injection control in these experiments. mRNA was transcribed using Megascript™ (Ambion, Austin, TX) and tailed using a Poly (A) Tailing Kit™ (Ambion, Austin, TX).

2.2. Morpholinos

A 25-mer antisense morpholino (5'-GCTTTCCGCAGACATGACTCGCAGC-3') was designed against the 5' UTR of *Xenopus ISWI* immediately adjacent to the translation start

(Gene Tools, LLC, Philomath, OR). Per Gene Tools recommendations, morpholinos were resuspended at 1 mM and injected into embryos to give final concentrations in the range of 1–10 μ M (10 μ M–80 ng total injected morpholino). A sample of morpholino was also lyophilized and resuspended at 2 mM for high concentration injections. For a control, we use a standard control 25-mer (5'-CCTCTTACCTCAGTTA CAATTTAT-3') available from Gene Tools, LLC (Philomath, OR). This oligo has no target (except in reticulocytes from thalassemic humans with a specific β -globin mutation) and is a commonly used negative control in antisense morpholino experiments. A 25-mer antisense morpholino (5'-GGCGTAGCCATC-TAATGTTCTGGAG-3') was also designed against *xbrm* (*Xenopus brahma*).

2.3. Mutagenesis

A dominant negative *ISWI* mutant was created using the mutagenic primers 5'GGCTGATGAAATGGGTCTAG-GAGCGACTTTGCAGACC-3' and 5'GGTCTGCAAA-GTCGTCCTAGACCCATTCATCAGCC-3', converting the lysine (underlined) at position 612 to an alanine. Mutagenesis was performed using Quickchange™ (Sigma, St Louis, MO).

2.4. Microinjection

Adult *Xenopus* were purchased from Xenopus Express (Plant City, FL). Embryos were obtained by in vitro fertilization and microinjection into the one cell stage was carried out by standard methods (Sive et al., 2000). Embryos were injected with 2, 4 or 10 ng of antisense RNA, or with 40, 80 or 160 ng of morpholino (the manufacturer suggested 80 ng as a starting concentration). GFP mRNA was injected at 10 ng. All injections were in a total volume of 10 nl. Embryos were incubated at 16 °C for 24–48 h and staged according to Nieuwkoop and Faber (Nieuwkoop and Faber 1967). Extensive GFP staining was observed throughout embryos in which *GFP* mRNA was injected, indicating that diffusion of injected material from the injection site was not a problem.

2.5. Protein isolation and immunoblotting

Protein was collected at stage 12/13 according to Merzdorf and Goodenough (1997). A final concentration of 1 μ M PMSF was added to the protein isolation buffer, and DIFP, chymostatin and Trasylol were omitted from this buffer. Samples were then run on an SDS-page gel and transferred using standard methods (Sambrook et al., 1989). Dr Paul Wade generously provided *ISWI* antibody. E-Cadherin antibody (5D3) was obtained through the Developmental Studies Hybridoma Bank at the University of Iowa (Iowa City, IA).

2.6. Whole mount in situ hybridization

Albino embryos were collected after in vitro fertilization and fixed in MEMFA according to Sive et al. (2000). Embryos were then rehydrated and assayed according to Sive et al. (2000) with the following changes: RNase step was omitted, and a second pre-antibody incubation step with 2% BMB blocking reagent and 20% sheep serum in MAB for 1 h@room temperature was added. AP buffer minus 2 mM levamisol was used as detection buffer. NBT/BCIP was used for the detection method.

2.7. Histology

Fixed embryos were dehydrated through a graded series of ethanol and xylene, embedded in Paraplast Plus (Oxford Labware, St Louis, MO) and serial sectioned at a thickness of 7 μ m. Sections were collected on albumin-subbed slides (Mayer's fixative (Humason, 1972). Sections were stained using Ehrlich's hematoxylin and counterstained in Eosin following the protocols of Humason (1972). Coverslips were applied using Permount (Fisher Scientific, Pittsburgh, PA). Color images were captured using a Spot digital camera (Diagnostic Instruments, Inc., Sterling Heights, MI).

2.8. RT-PCR

Total RNA was isolated using RNeasy™ (Qiagen). One step real-time RT-PCR was performed using Lightcycler™ reagents and the Cepheid Smartcycler (real time PCR). Reactions contained 1 μ g total RNA and 2.5 pmol of primer, and were subjected to 25 cycles. Annealing temperatures were optimized for each primer set. Products were detected using Cyber Green during the real-time PCR reaction and/or running the final products on a 1% agarose gel. PCRs were performed a minimum of three times with samples from independent injection experiments. Primers were obtained through Sigma Genosys (St Louis, MO). Primer sequences for *Hoxb9*, *MyoDb*, *EF1 α* , and *NCAM* were obtained through Xenbase (www.xenbase.org). *Xmeis1b* was previously described (Maeda et al., 2001). Sequences for other primers are as follows:

BMP4: 5'-CCATGCCAGCCTCATACC-3' + 5'-GCTG-GTCGGTCTCTCAGG-3'

Shh: 5'-GGTTCGACTGGGTCTATTACG-3' + 5'-CG-ATGAACATGAGGAAGTCG-3'

Slug: 5'-GGACTTAACCTCCTGCAGG-3' + 5'-GGAT-CGTTGCTGGATTGTCTAGG-3'

Sox9: 5'-GGAGACTTCTGAATGAGGG-3' + 5'-GCT-GGATATCTGTCTTGGG-3'

Pax6: 5'-CCGAGAAATGTCGCAGGG-3' + 5'-GGAA-TTACACAGTCCCTGGG-3'

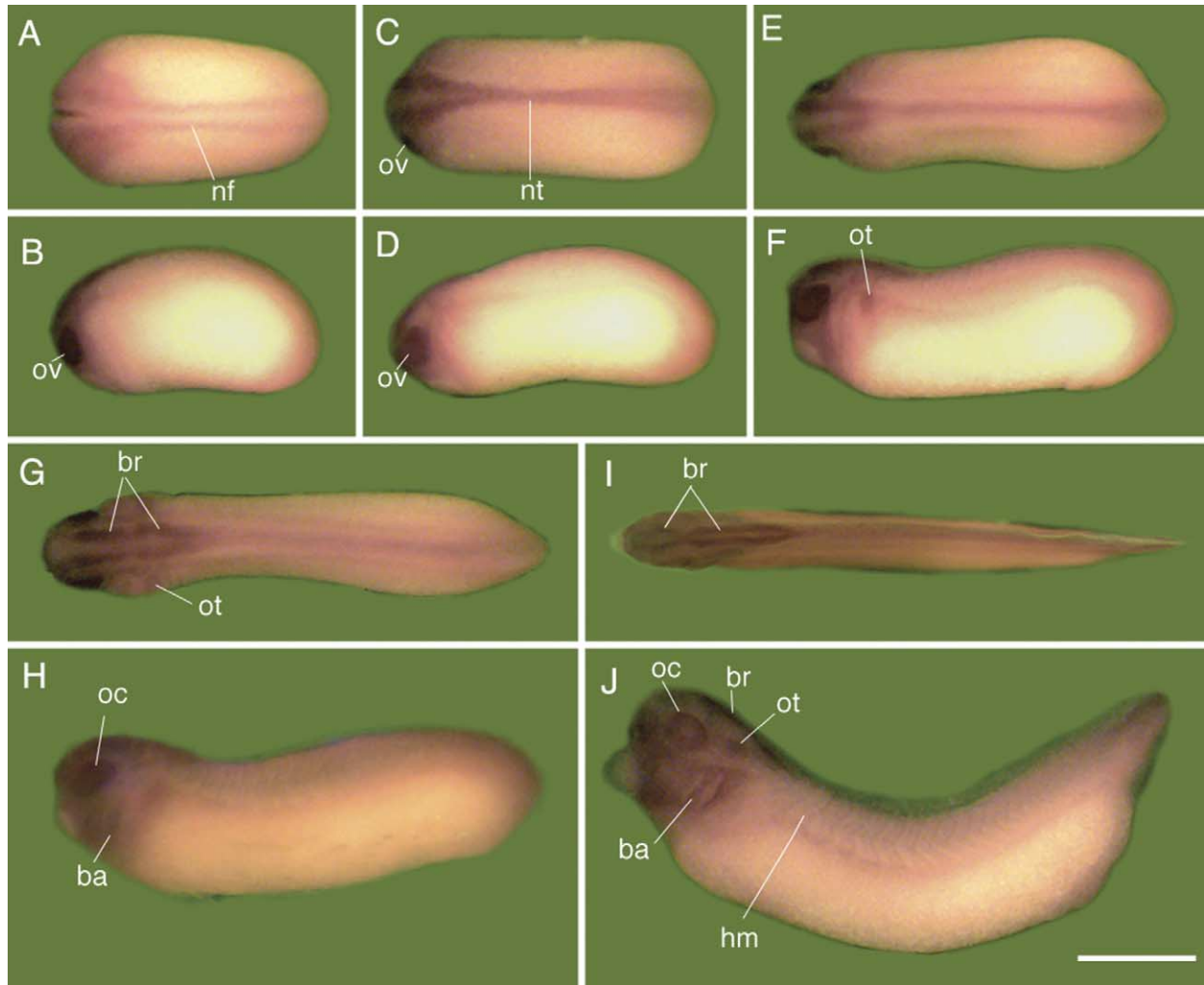


Fig. 1. Whole mount in situ hybridization of *Xenopus* embryos with a 343 bp *ISWI* digoxigenin-labeled probe. A–J: Corresponding dorsal and left lateral views of stage 18 (A–B), 24 (C–D), 26 (E–F), 28 (G–H) and 33 (I–J) embryos showing expression of *ISWI* in regions of the neural tube, brain, and optic vesicles. All embryos are oriented with the anterior end towards the left side of the figure. nf, neural fold; nt, neural tube; ov, optic vesicle; ot, otic vesicle; oc, optic cup; br, brain; ba, brachial arches; hm, hypaxial muscles. Scale bar equals 1 mm.

2.9. Chromatin immunoprecipitation

Groups of 100 embryos were fixed in MEMFA (0.1 M Mops pH 7.5, 2 mM EGTA, 1 mM MgSO₄, 3.7% formaldehyde) for 30 min, rinsed briefly and homogenized in lysis buffer (1% SDS, 10 mM EDTA, 50 mM Tris-HCL pH 8.1, 1 µl/ml Leupeptin, 1 mM PMSF, 1 µl/ml Pepstatin). Homogenized embryos were passed through a 20-gauge needle (20 passes). Chromatin was sonicated to yield DNA fragments between 200 and 500 bp. Debris was removed by centrifugation for 10 min at 5000 rpm@4 °C, supernatant was collected and spun again. DNA was quantified by measuring the absorption at 260 nm. Each sample was then diluted to 0.1 µg/µl in lysis buffer. Subsequent steps were performed as described (Krebs et al., 1999). Input and immunoprecipitated material was detected via slot blot.

3. Results

3.1. *Xenopus ISWI* is expressed in neural tissues

Two nearly identical *ISWI* genes have been isolated from *Xenopus*, *ISWI 1* (Demeret et al., 2002) and *ISWI 2* (Guschin et al., 2000), which differ only by a nine amino acid stretch that is not present in *ISWI 2* (amino acids 179–188 of *ISWI 1*). Probes and antibodies that detect both *ISWI*s reveal that *ISWI* is maternally deposited in the oocyte, and is also expressed continuously throughout embryonic development (Demeret et al., 2002), though localization of expression was not addressed in that study.

As a first step in determining the function of *ISWI* in *Xenopus*, we performed in situ hybridization in whole-mount embryos to determine the patterns of expression of *ISWI* in different developmental stages. The in situ probe

recognizes both *ISWI 1* and *ISWI 2*. The pattern of *ISWI* staining in selected stages (stages 18–33) is shown in Fig. 1A–J (see also Fig. 2D–F). Our results indicate that *xISWI* mRNA is localized to neural tissues throughout development. Specifically, *ISWI* is detected in the neural folds, in the cranial crest/brachial arches, in the otic vesicle, and to some extent in the migrating hypaxial muscles in early embryos. In later stages, *ISWI* is expressed throughout the brain and spinal cord. *ISWI* also exhibits strong eye

staining in all stages. These results were surprisingly analogous to the recent findings that xBaf57 (a homolog of a subunit of mammalian and *Drosophila* SWI/SNF complexes) increases the expression of neural markers in ectoderm explants and is expressed in mesoderm during gastrulation and the nervous system during the neurula and tailbud stages of the *Xenopus* embryo (Domingos et al., 2002). The fact that two different remodeling complexes are involved in nervous system development is very intriguing.

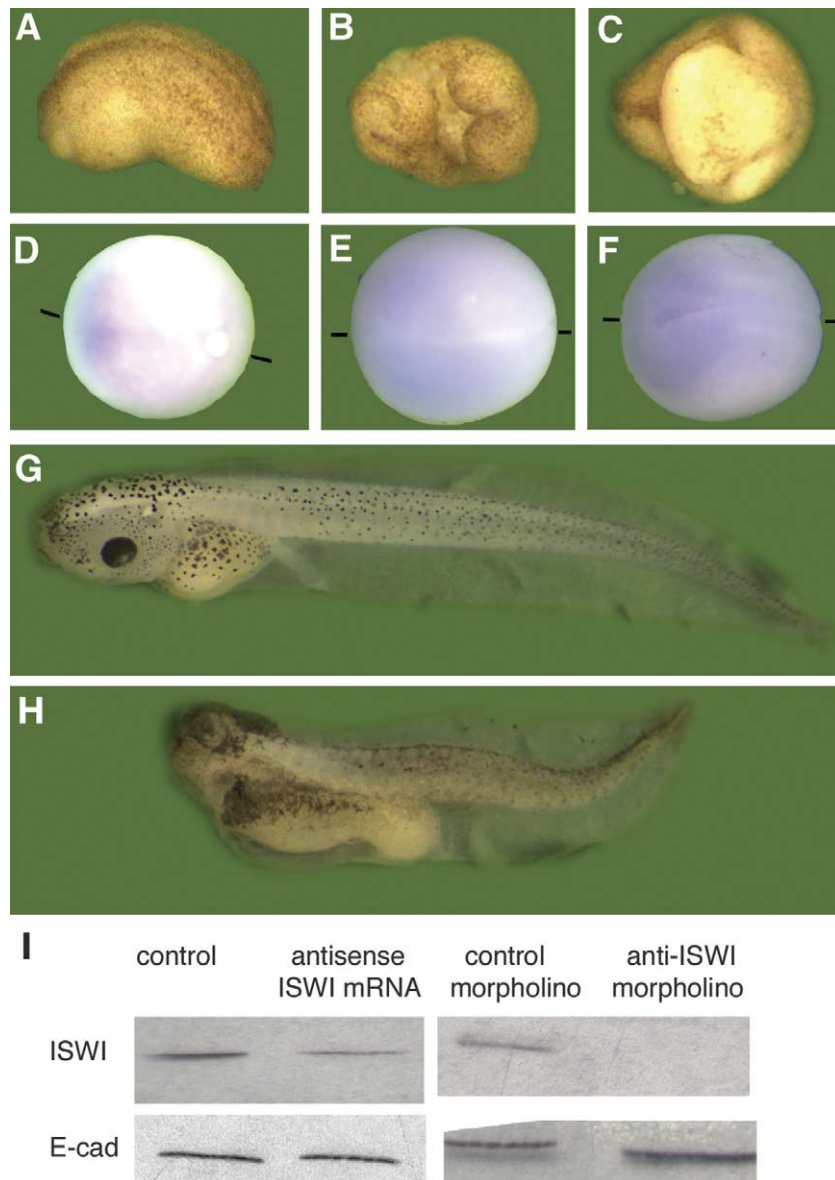


Fig. 2. *Xenopus laevis* embryos injected with antisense *ISWI* RNA or anti-*ISWI* morpholino. A–C: Embryos photographed when control-injected embryos reached approximately stage 20–22. Embryos were injected with either 80 ng control morpholino (A), 4 ng of antisense *ISWI* RNA (B; representative of phenotype observed for injection of 2 and 10 ng as well) or 80 ng anti-*ISWI* morpholino (C; also representative of other of 40 and 160 ng morpholino injections). D–F: Whole mount in situ hybridization of stage 12 (D), 13 (E) and 14 (F) embryos with the *ISWI* probe described in Fig. 1, showing early differential expression of *ISWI*. These are dorsal views with the anterior to the left side of the figure. Black dashes indicate the midline for each embryo. G–H: Embryos injected with 80 ng of either control morpholino (G) or anti-*ISWI* morpholino (H). The embryo in H represents one of the very few embryos to survive the initial gastrulation defect at high morpholino concentrations. I: Western blot showing reduced levels of *ISWI* protein in embryos injected with 10 ng of *ISWI* antisense RNA (left), or 80 ng anti-*ISWI* morpholino (right), compared to control embryos injected with nanopure water or control morpholino (80 ng), respectively. Antibody against E-cadherin (E-cad) is used as a loading control.

A recent comprehensive survey of expression of SWI2/SNF2 family members in tailbud-stage embryos revealed that in fact all SWI2/SNF2 family members are expressed to varying extents in the brain, but exhibit greatly varying expression patterns in other tissues, including other neural tissues (Linder et al., 2004). Note that the in situs described by Linder et al. and in this work do not distinguish the localization of the two different *ISWI* transcripts, which is technically difficult to accomplish.

3.2. *xISWI* expression is required for normal gastrulation and neural development

To determine the function of *ISWI* in *Xenopus* development, either a 300 bp antisense *ISWI* RNA or an anti-*ISWI* morpholino was injected into fertilized eggs to inhibit translation of endogenous *ISWI* mRNA. Eggs were injected with 2, 4 or 10 ng of RNA or 40, 80 or 160 ng of morpholino. While some studies have obtained results with lower concentrations of morpholinos, this concentration range was chosen according to the manufacturer's recommendations and is consistent with other published studies (Audic et al., 2001; Khokha et al., 2005). For controls, eggs were injected with 10 nl of water, 10 ng of *GFP* mRNA, or 40, 80 or 160 ng of a control morpholino (see Tables 1 and 2). Embryos were allowed to develop at 16 °C. Representative injected embryos are shown in Fig. 2A–C, G and H.

At approximately 30 h post-fertilization, when control embryos had reached stages 18–22 (Fig. 2A), an interesting phenotype began to emerge. Anti-*ISWI* injected embryos showed widespread failure of gastrulation and disruption of neural tube closure (Fig. 2B, antisense *ISWI* RNA-injected embryo; Fig. 2C, anti-*ISWI* morpholino-injected embryo). At the highest doses of antisense or morpholino, close to 90% of the embryos exhibited these defects, compared to only 13–15% gastrulation failure in the equivalent control injections (Table 1). Injection of 80 ng of the control morpholino does not significantly affect development (e.g. Fig. 2G, embryo injected with control morpholino).

Although, it was already known that *ISWI* is present in the oocyte and throughout early development (Demeret et al., 2002), the early defects in gastrulation and neurulation led us to wonder whether *ISWI* is already exhibiting differential expression at these early stages. We therefore performed in situ hybridizations in embryos between stages 10 and 14. Representative in situs are shown in Fig. 2D–F. *ISWI* stains diffusely throughout the dorsal half of stage 10 embryos (not shown), but begins to localize to the anterior end by stage 12 (Fig. 2D), and shows clear neural plate and neural fold staining in stages 13/14 (Fig. 2E, F). This confirms that *ISWI* expression is rapidly localized to presumptive neural tissue early in development, consistent with the early critical role revealed in the antisense/morpholino injections.

A percentage of antisense- or morpholino-injected embryos survive the early defects and go on to reveal later

Table 1
Neural phenotypes in injected embryos

	Amount injected (ng)	Total no. of embryos	No. of embryos with neural defects ^a	% of embryos with neural defects ^a
Uninjected		1252	31	0.02
Water		998	89	9
GFP mRNA	10	1117	167	15
Control MO	40	573	81	14
	80	538	21	4
	160	484	61	13
Anti- <i>ISWI</i> mRNA	2	933	434	47
	4	599	452	75
	10	500	442	88
Anti- <i>ISWI</i> MO	40	689	228	33
	80	575	488	85
	160	284	253	89
DN- <i>ISWI</i> mRNA	10	631	507	80
DN- <i>ISWI</i> mRNA + WT <i>ISWI</i> mRNA	10+5	148	63	43
DN- <i>ISWI</i> mRNA + WT <i>ISWI</i> mRNA	10+10	229	77	33
DN- <i>ISWI</i> mRNA	5	202	109	54
WT <i>ISWI</i> mRNA	5	142	28	80
DN- <i>ISWI</i> mRNA + WT <i>ISWI</i> mRNA	5+5	267	41	15

^a Includes failure of gastrulation, neural tube closure, brain, eye and spinal deformities.

developmental abnormalities. The example shown in Fig. 2H illustrates an anti-*ISWI* morpholino-injected embryo (80 ng) at approximately stage 40 (compare to the control morpholino-injected embryo in panel G). This embryo exhibits spinal deformities and dramatically reduced brain and eye development. At lower doses of *ISWI* inhibition (e.g. 40 ng of anti-*ISWI* morpholino), more embryos survive the early gastrulation defects and go on to

Table 2
Cataract formation in injected embryos

	Amount injected (ng)	Total no. of embryos	No. of embryos with cataracts	% of embryos with cataracts (%)
GFP mRNA	10	97	0	0
Control MO	80	273	0	0
Anti- <i>ISWI</i> MO	80	150	133	89
DN- <i>ISWI</i> mRNA	10	109	83	76

exhibit a spectrum of later neural defects, including severe eye defects, described below.

To confirm that ISWI translation was specifically inhibited in these embryos, we isolated total protein from stage 12 embryos that were injected with either 10 ng antisense *ISWI* RNA or 80 ng anti-*ISWI* morpholino. Total protein was also isolated from water or control-morpholino (80 ng) embryos at the same stage. The protein was run on an SDS-page gel and screened by western blot for ISWI protein, using an anti-ISWI antibody generously provided by Dr Paul Wade (Emory University, Atlanta, GA). Processed ISWI protein runs at about 137 kDA. Western analysis reveals that ISWI protein levels are reduced but not eliminated in the antisense-injected embryos (Fig. 2F, left). In contrast, ISWI was completely undetectable in the morpholino-injected embryos (Fig. 2F, right). For loading controls, we used both Coomassie staining (not shown) and detection of E-cadherin protein, which was detected at similar levels in all samples. This clearly indicates that both the antisense *ISWI* RNA and the anti-*ISWI* morpholino are successfully reducing or preventing the translation of endogenous *ISWI* mRNA.

The consistency between the phenotypes observed for both antisense RNA and morpholino methods strongly suggest the defects are due to the specific loss of ISWI (and not the result of non-specific toxicity of the anti-*ISWI* morpholino), and the western data supports this conclusion. A third method of ISWI inhibition using a dominant negative approach yields the same results (see Fig. 4B–D, discussed below). In addition, we have also designed a morpholino that inhibits expression of *xbrm* (*Xenopus brahma*), a SWI2/SNF2-family member related to *ISWI*. This morpholino, injected at the same concentrations as the anti-*ISWI* morpholino, does not result in gastrulation or neural defects but rather in later developmental defects unrelated to the defects observed in *ISWI*-deficient embryos (E.E. Brown, S.S.D. and J.E.K., unpublished results).

3.3. *xISWI* is required for normal expression of neural genes

Formation of the central nervous system (CNS) in vertebrates is initiated during gastrulation and depends on the inductive interaction of the ectoderm and the adjacent dorsal mesoderm. The CNS is characterized by overt anteroposterior (AP) and dorsoventral patterning (Doniach, 1993; Mathis and Nicolas, 2002). Nieuwkoop has described the predominant concept of how AP patterning is formed in a two-step model (Nieuwkoop, 1999). The first step, ‘activation,’ is thought to specify anterior neuroectodermal structures, such as the forebrain. The second step is ‘transformation’ where anterior neural tissue is respecified to more posterior fates such as midbrain, hindbrain and spinal cord. A number of genes have been identified whose regulation is critical in this process (Weinstein and Hemmati-Brivanlou, 1999; Knecht and Bronner-Fraser, 2002).

Many ATP-dependent chromatin remodelers have been shown to act by regulating transcription, both positively and negatively. To determine whether ISWI controls expression of genes involved in neural development, we initiated a search for specific gene targets of ISWI. We tested whether expression of a number of known neural and associated tissue marker genes was affected in the injected embryos. Total RNA was purified from the antisense- or morpholino-injected embryos (4 and 80 ng, respectively) and subjected to RT-PCR using primers against a variety of neural markers expressed at different times and positions in neural development. These include *BMP4* (bone morphogenic protein4; an inhibitor of neural tissue formation that is expressed throughout the late blastula and is down-regulated in neural tissue at approximately stage 10), *Xmeis* (a pre-pattern neural crest marker that is expressed with the down-regulation of *BMP4*), *Shh* (sonic hedgehog; an early notochord marker expressed at gastrulation), *Pax6* (a key regulator of eye development expressed continuously from stage 14), *NCAM* (neural cell adhesion molecule; expressed in most neural tissue at the start of gastrulation), *Sox9* (a progenitor of cranial neural crest formation, expressed at the start of gastrulation and persists through early development), *Slug* (a neural crest and lateral plate marker expressed at the start of neurulation), and *HoxB9* (a central nervous system marker is expressed at early to mid neurula stage). As controls, we also detected the expression of the muscle-specific *MyoD* gene and the gene encoding the ubiquitously expressed translation protein EF1 α .

We performed real-time RT-PCR on samples from both antisense RNA- and anti-*ISWI* morpholino-injected embryos (4 and 80 ng, respectively). The results were the same for both; data for the morpholino injections are shown in Fig. 3. Fig. 3A shows representative PCR products from the RT-PCR reactions. The average level of expression for each gene in the *ISWI* knockdown embryos is expressed as a percentage of the level of expression in control-injected embryos (Fig. 3B). Each bar represents the data from a minimum of three separate injection experiments, and standard errors are shown.

Xmeis, *Shh*, *Pax6*, *NCAM*, *Sox9*, *Slug* and *HoxB9* all show a decrease in expression compared to embryos injected with water, GFP mRNA (10 ng) or control morpholino (80 ng) (Fig. 3 and data not shown), suggesting that ISWI is acting at a very early step in this developmental cascade, which is consistent with the gastrulation defect we observe. The muscle-specific *MyoD* was unaffected by the presence or absence of ISWI, supporting the hypothesis that the primary role of ISWI is in the development of neural tissue.

3.4. *ISWI* binds directly to the *BMP4* promoter

Consistent with the down-regulation of neural genes, expression of *BMP4* was increased approximately 2-fold in anti-*ISWI* morpholino-injected embryos (Fig. 3A, B).

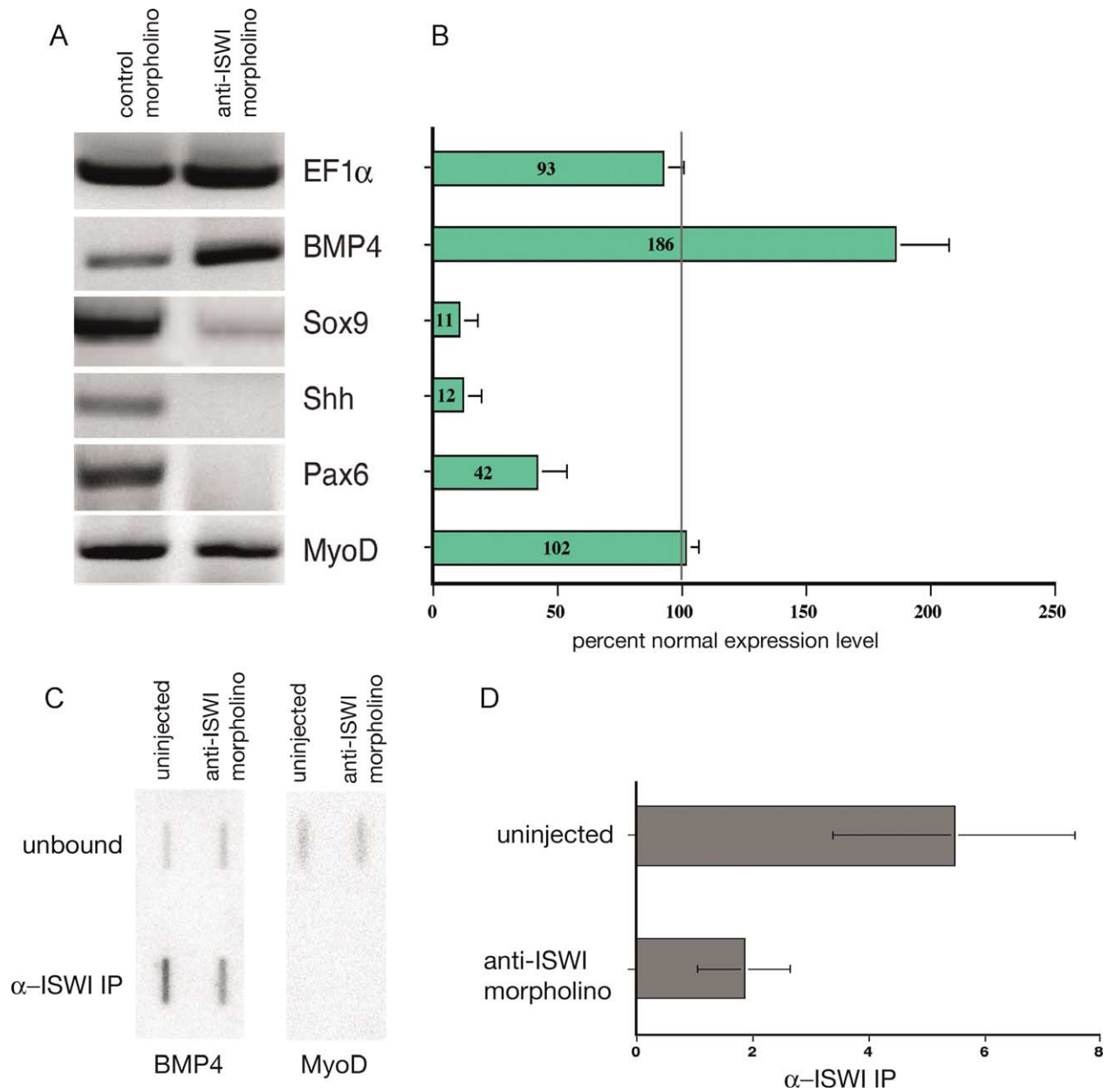


Fig. 3. RT-PCR of tissue-specific genes in anti-*ISWI* morpholino-injected embryos. Total RNA was collected from embryos at the specified stages and real-time RT-PCR was performed with specific neural gene primers. (A). Products of RT-PCR reactions. *EF1α* was tested at stages 10, 12, 13, 15, 18 and 20. The stage 13 data is shown and is representative of all stages tested. Other genes shown were analyzed at the following stages: *BMP4*, stage 10/11; *Sox9* and *Shh*, stage 13; *Pax6* and *MyoD*, stage 15/16; *HoxB9*, stage 18/20. (B). Quantitative data from real-time RT-PCR, showing the level of expression (as percentages) of each gene compared to the levels in control-injected embryos. Each bar represents the average from a minimum of three injection experiments. Standard errors are shown. (C). Representative slot blots of chromatin immunoprecipitations with anti-*ISWI* antibody. Chromatin was extracted from stage 12/13 embryos; comparable results were obtained with later stages. Left panel was probed for *BMP4*, right panel was probed for *MyoD*. (D). Average enrichment of *ISWI* at *BMP4* in uninjected and anti-*ISWI* MO-injected embryos (80 ng) (stage 12/13). Standard errors are shown.

Reduced BMP activity has been shown to induce anterior-neural tissue from non-neural ectoderm (Harland and Gerhart, 1997). *BMP4* is normally down-regulated in neural tissue in order for neurulation to begin.

Since *ISWI* has been implicated in both activation and repression of genes, we wished to test whether *ISWI* is directly targeted to the *BMP4* promoter, where it could act as a repressor in neural tissues. We therefore used chromatin

immunoprecipitation (ChIP) analysis to detect *ISWI* protein at *BMP4*. We used the anti-*ISWI* antibody to immunoprecipitate cross-linked, sheared chromatin, and measured the enrichment of *BMP4* or control sequences (*MyoD*) using slot blots. Representative blots are shown in Fig. 3C, and the average enrichment of *ISWI* at *BMP4* is shown in Fig. 3D. *ISWI* protein is detected at *BMP4* in vivo (Fig. 3C, left) consistent with a direct role for *ISWI* in *BMP4* regulation.

In contrast, no ISWI is detected at the *MyoD* gene, the expression of which is unaffected by the presence or absence of ISWI (Fig. 3A, B). Furthermore, the *BMP4* signal is lost in anti-ISWI morpholino-injected embryos.

These results strongly suggest that ISWI acts as a repressor of *BMP4* in neural tissue. This analysis was performed in whole embryos; ChIPs of neural vs. non-neural tissue will help confirm whether ISWI is a repressor of *BMP4* in neural tissue or an activator of *BMP4* in other tissues in future studies.

3.5. A dominant-negative ISWI mutant also inhibits development

Antisense interference using direct injection of antisense RNA or morpholinos is a powerful method for functional inhibition of a target gene in all tissues in early development. However, it is more difficult to target injected antisense/morpholinos to specific tissues. We have developed a dominant-negative mutant of α ISWI, *DN-ISWI*, which can ultimately be placed under the control of tissue-specific or inducible promoters in transgenic frogs. We identified the invariant lysine in the ISWI ATPase domain (K612) and mutated it to an alanine (Fig. 4A). The mutation was confirmed through sequencing and the plasmid was named ISWI-K612A. Mutation of this conserved lysine has been used to create catalytically inactive mutants of yeast *SWI2* (Khavari et al., 1993; Richmond and Peterson, 1996) and human *Brg1* and *hbrm* (de la Serna et al., 2001). These ATPase Δ mutants assemble into remodeling complexes, competing with the wild-type ATPase for complex assembly.

To confirm that the ISWI-K612A mutant behaves as a dominant negative in *Xenopus* embryos, we tested whether the presence of the mutant *ISWI* in early embryos could recapitulate the phenotype we observed in the antisense-/morpholino experiments. A 3500 bp *DN-ISWI* transcript was produced using the T7 promoter and a poly-A tail was added for better translation efficiency. A *GFP* transcript was also synthesized as a control for the effects of injecting any tailed mRNA. After injection of *DN-ISWI* or *GFP* mRNA, embryos were allowed to develop at 16 °C.

Injection of the *DN-ISWI* mutant mRNA results in gastrulation and neural fold phenotypes that are indistinguishable from those observed in the antisense- and morpholino-injected embryos (Fig. 4B). *DN-ISWI* protein is strongly expressed in embryos as measured by Western analysis (data not shown). As we observed with antisense RNA and morpholino injections, injection of lower concentrations of *DN-ISWI* mRNA permitted a number of embryos to survive the early gastrulation defects, allowing us to detect phenotypes at later stages. Comparable to the morpholino-injected embryos, *DN-ISWI* mRNA-injected embryos exhibit a spectrum of defects in brain and eye development. These include extreme developmental delays in eye development: for example, at stages 35–38,

ISWI-deficient embryos had small, flattened lenses still attached to the overlying ectoderm (separation normally occurs at stage 33), resembling lens placodes as normally seen at stage 25–26.

Another dramatic phenotype is shown in Fig. 4C. Some embryos injected with *DN-ISWI* mRNA exhibit a catastrophic failure of forebrain development, coupled with malformed eyes that are mislocalized to the central axis of the animal, essentially occupying the space created by the reduction of forebrain tissue.

To show that *DN-ISWI* is in fact acting as a dominant negative, we performed a rescue experiment in which wild-type *ISWI* mRNA was coinjected with the *DN-ISWI* mRNA, in order to provide more wild type *ISWI* to compete with the dominant negative mutant. The neural phenotype caused by the injection of *DN-ISWI* can be rescued by co-injection with wild type *ISWI* mRNA (Table 1). Coinjection of 10 ng *DN-ISWI* + 5 ng wild type *ISWI* resulted in a two fold-reduction of the mutant phenotype to only 43% of the injected embryos, compared to a neural phenotype in 80% of the embryos injected with *DN-ISWI* alone. Coinjection of 10 ng of both *DN-ISWI* and wild type *ISWI* reduces the neural phenotype to only 33% of the injected embryos.

We also wished to confirm that the *DN-ISWI* could produce the same transcriptional defects observed with the antisense or anti-*ISWI* morpholino injections shown in Fig. 3A, B. Importantly, we wanted to show that these transcriptional defects could be rescued by co-injection of wild-type *ISWI* mRNA. For this experiment, we injected either 5 ng of *DN-ISWI* or wild-type *ISWI* mRNA alone, or co-injected 5 ng each of *DN-ISWI* and wild-type *ISWI* mRNA. We chose to inject only 5 ng of *DN-ISWI* mRNA to ensure that sufficient embryos would survive past stages 10–12 to allow transcriptional analysis during stages 13–18 (as was done in Fig. 3A, B). Five nanogram of *DN-ISWI* mRNA resulted in neural phenotypes in 54% of the embryos, and co-injection of the wild-type mRNA rescued this defect (only 15% of embryos with neural defects; see Table 1).

Fig. 4E shows the results of the RT-PCR analysis of these injected embryos. The *DN-ISWI* produced the same pattern of transcriptional defects as the antisense or anti-*ISWI* morpholino: *BMP4* transcripts were increased, *Sox9*, *Pax6* and *Shh* transcripts were decreased, and transcription of *MyoD* was unaffected relative to control embryos. Furthermore, co-injection of wild-type *ISWI* mRNA partially rescued the *Sox9*, *Pax6* and *Shh* transcriptional defects, and fully rescued the *BMP4* overexpression.

Taken together, these results confirm that it is the loss of *ISWI* function that results in the developmental and transcriptional defects observed. It is also important to note that the fact that *DN-ISWI* causes the same phenotypes as inhibition of *ISWI* translation suggests that it is the chromatin remodeling/ATPase activity per se of *ISWI* that is critical for its function in development.

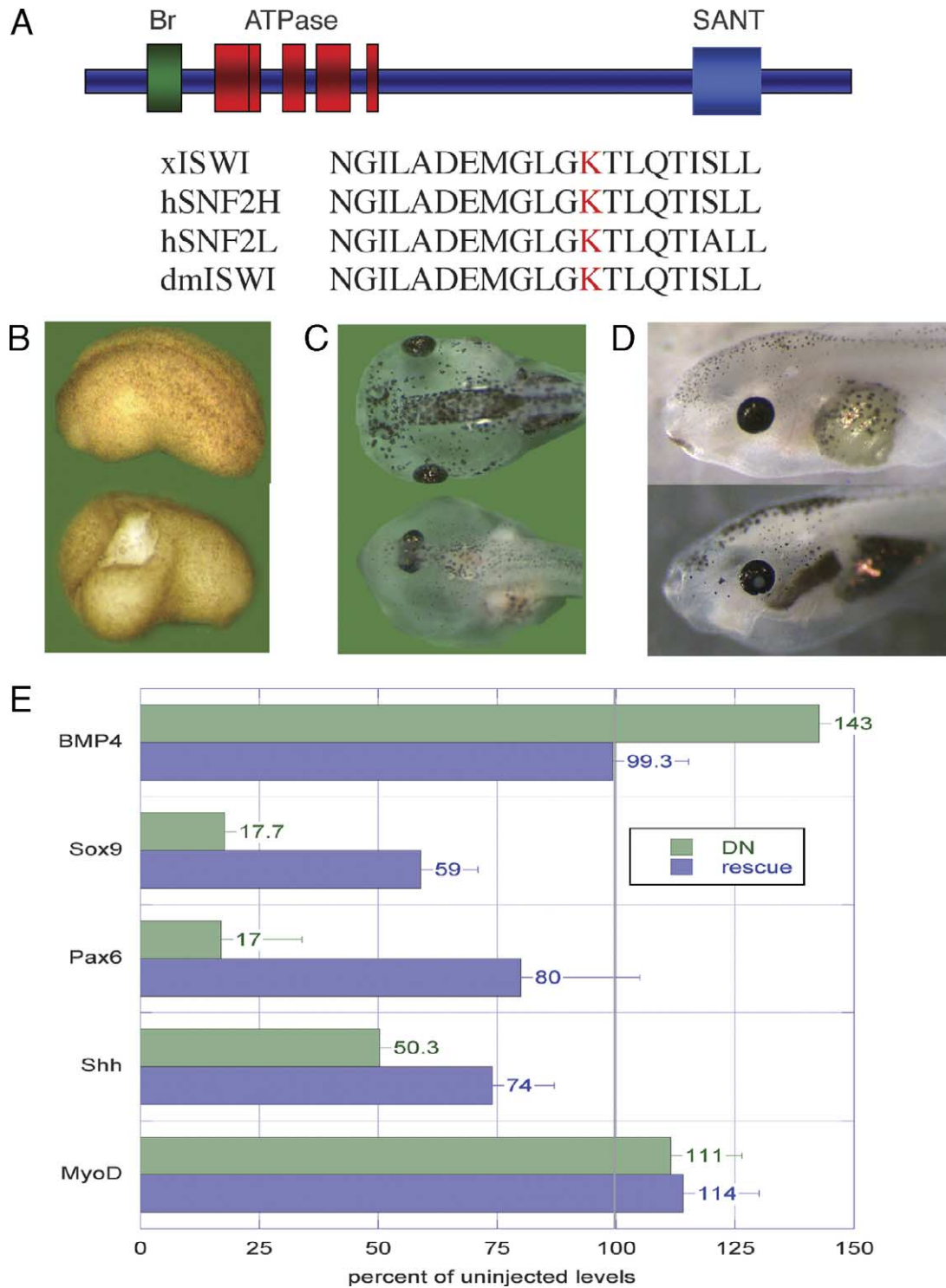


Fig. 4. An ATPase mutant of ISWI acts as a dominant negative in vivo. (A). The conserved lysine in the *Xenopus* ISWI ATPase domain, which is essential for ISWI's catalytic activity, was located and mutated to an alanine. An alignment of *Xenopus*, human, and *Drosophila* ISWI homologs shows the relevant region, with the invariant lysine (K) shown in red. (B). Injection of 10 ng *DN-ISWI* mRNA recapitulates the gastrulation defect observed in antisense- or anti-*ISWI* morpholino-injected embryos (bottom panel). Top panel shows a control embryo injected with 10 ng *GFP* mRNA. (C). Failure of brain development in *DN-ISWI* mRNA-injected embryo (bottom); compare to stage 45 embryo from same egg clutch injected with *GFP* mRNA (top). (D). Cataract development in stage 43 embryo injected with *DN-ISWI* mRNA (bottom; gray spot in center of eye); control *GFP* mRNA-injected embryo is shown above. (E). Quantitative data from real-time RT-PCR, showing the level of expression (as percentages) of each gene compared to the levels in control-injected embryos. The green bars ('DN') represent data from embryos injected with 5 ng *DN-ISWI* mRNA, the blue bars ('rescue') represent embryos co-injected with 5 ng each of *DN-ISWI* and wild-type *ISWI* mRNA. Genes shown were analyzed at the following stages: *BMP4*, stage 10/11; *Sox9* and *Shh*, stage 13; *Pax6* and *MyoD*, stage 15/16. Each bar represents the average from three injection experiments. Standard errors are shown.

3.6. ISWI-deficient embryos develop posterior subcapsular cataracts and have defects in retinal differentiation

Late stage survivors of *DN-ISWI* mRNA injections develop a striking phenotype at approximately stage 38/40: the development of congenital cataracts in the vast majority of the survivors (Fig. 4D; Table 2). This phenotype also occurs in anti-*ISWI* morpholino-injected embryos; in some batches of injected embryos every survivor eventually developed clouded lenses, while the cataract phenotype never appeared in control injections (Table 2). In addition, these embryos appear to be blind, in that they are unresponsive to shadows or objects moving above them, stimuli that cause control embryos to swim rapidly away from the objects, substantiating the extent of these lens and retinal defects. The cataractous embryos do, however, respond to currents or touch, consistent with specific visual impairment.

There are many different types of congenital cataracts, such as those identified in humans (Amaya et al., 2003). We

therefore performed histological analyses to further characterize the specific eye defects in the *ISWI*-deficient embryos. Sections from both control and anti-*ISWI* morpholino-injected embryos at stages 38 and 45 are shown in Fig. 5A–F.

The cataractous lenses exhibit abnormal cell proliferation on the posterior surface, leading to the accumulation of large densely stained, basophilic cells (Fig. 5E, asterisk) resulting in a form of posterior subcapsular cataract and a severe lenticonus condition. Liquefied, apoptotic cells also appear to be present.

In general the *ISWI* morpholino knockdown eyes appear to be retarded in their development when compared to control eyes. Anti-*ISWI* morpholino-injected embryos exhibit defects in retinal differentiation, and cell adhesion (compare Fig. 5A, C–D and F). Younger stage 38 eye cups appear to have many loose rounded cells. Some cells in the younger embryos also appear to be picnotic, highly condensed, fragmented and apoptotic (Fig. 5D). Later defects are also apparent. For instance, cells of the ganglion

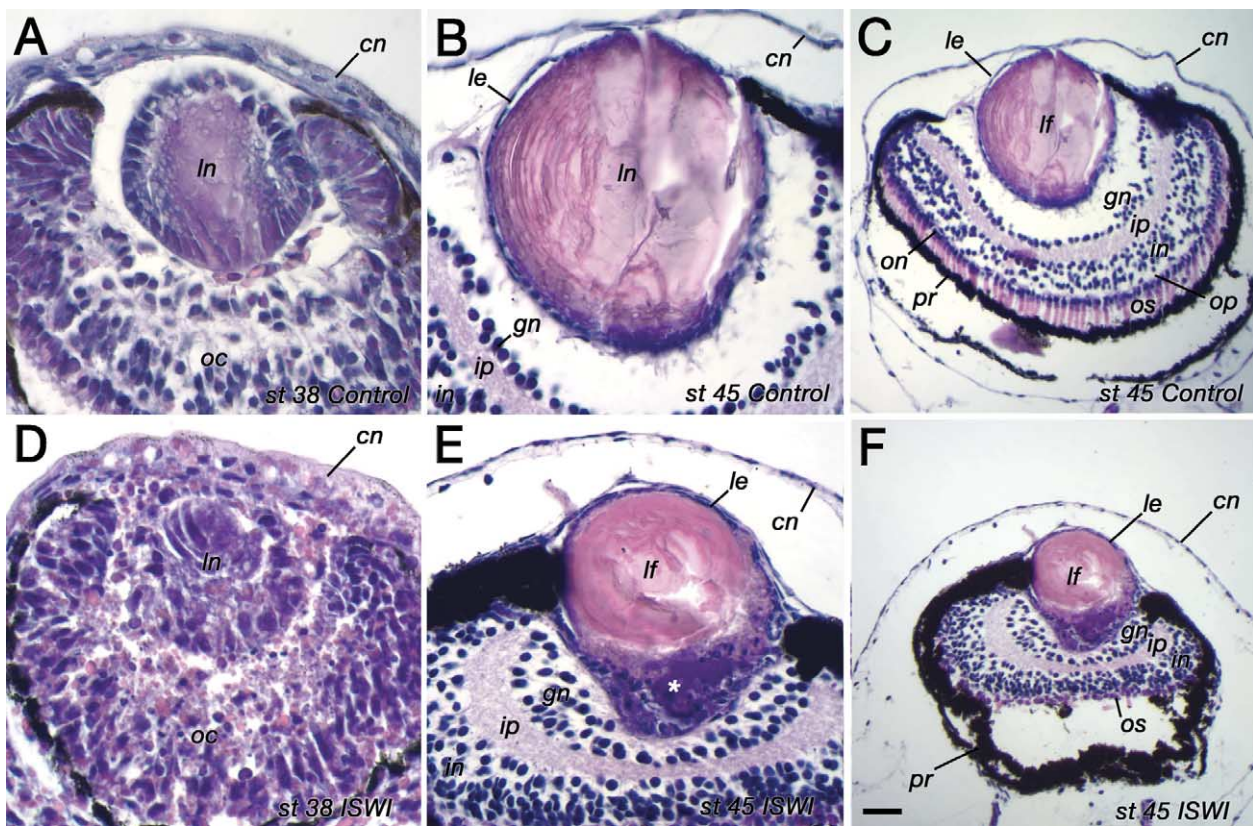


Fig. 5. Cross-sections through normal control and defective eyes in *ISWI* morpholino knockdown embryos. (A). Normal stage 38 eye showing optic cup, lens and cornea. Note presence of large central, primary lens fiber cell 'nucleus' and additional secondary lens fiber cells at the periphery of the lens. (B–C). Corresponding high and low magnification views of the normal eye in a stage 45 animal. Note large mass of enucleated lens fiber cells and thin nucleated lens epithelium. Also note normal arrangement of differentiated cell layers within the eye cup. D. Stage 38 *ISWI* morpholino knockdown eye. Note that the lens is more poorly developed compared to (A) and contains a much smaller mass of primary lens fiber cells. Other lens and retinal cells appear to be more highly rounded. E–F. Corresponding high and low magnification views of the stage 45 *ISWI* morpholino knockdown eye. Note presence of large basophilic, nucleated cell mass (cataract) on the posterior surface of the lens (asterisk). Defects are also apparent in the development of the retinal layers (see text for further details). Cn, cornea; gn, ganglion layer; in, inner nuclear layer; ip, inner plexiform layer; le, lens epithelium; If, lens fiber cells; In, lens; oc, optic cup; on, outer nuclear layer; op, outer plexiform layer; os, rod and cone outer segments; pr, pigmented retinal epithelium. Scale bar equals 25 μm for A–B and D–E, 50 μm for C and F.

layer do not appear to be arranged in a single layer (Fig. 5E, F). These cells are also closely associated with the lens, which is normally well separated at this time (compare Fig. 5B, E). There is no clear distinction of the inner and outer nuclear layers nor the formation of a thin outer plexiform layer (compare Fig. 5C, F). Furthermore, the rod and cone outer segments appear to be poorly developed in ISWI knockdown animals. Frequently, we observed that the retinal pigmented epithelium is detached from the rod and cone outer segments, suggesting that there may be other changes in cell adhesion, as well (compare Fig. 5C, F).

4. Discussion

We have shown that *Xenopus* ISWI mRNA is located specifically in neural tissue, including brain, neural fold, hypaxial muscle, the optic vesicle and cup, auditory vesicles and spinal cord. Early inhibition of ISWI protein production causes a lethal phenotype of incomplete gastrulation and neurulation. The mRNA levels of the neural-specific genes *Xmeis*, *shh*, *slug*, *sox9*, *Pax6*, and *Hoxb9* are greatly reduced in embryos injected with antisense ISWI RNA, anti-ISWI morpholino or dominant-negative ISWI mRNA, while the muscle-specific gene *MyoD* is unaffected. However, the mRNA of *BMP4*, a gene normally down-regulated in neural tissue as neurulation begins, is over-expressed in ISWI-deficient embryos. Both the developmental and transcriptional phenotypes caused by DN-ISWI mRNA injection can be rescued by co-injection of wild-type ISWI mRNA. We propose that ISWI may normally facilitate the formation of neural tissue by repressing genes that inhibit neural tissue such as *BMP4*, which is supported by the fact that ISWI binds directly to the *BMP4* gene in vivo, and this interaction is perturbed upon injection of anti-ISWI morpholino. This model does not exclude an additional role for ISWI in activating genes that specify neural tissue development. It is possible that ISWI has multiple neural-specific gene targets and is continuously required throughout development.

The knockdown of ISWI also results in the formation of congenital cataracts. ISWI is not normally expressed in the lens ectoderm. Hence, we surmise that these cataracts are due to the retarded and abnormal development of the retinal tissues in these embryos, leading to abnormal induction of the lens, and possibly to the inadequate production of key growth factors required to sustain normal lens development and differentiation. These lens defects could also stem from abnormal planar induction of the placodal ectoderm during the early phase of lens induction (Henry and Grainger, 1990). These effects may be directly or indirectly related to the abnormal regulation of *BMP4* expression in the neural ectoderm, or to other key genes involved in controlling and patterning eye development such as *Pax6* or *shh*. (Zuber et al., 2003; Marti and Bovolenta, 2002). For instance, it is known that *BMP4* plays a key role in eye development and lens induction (Furuta and Hogan, 1998). It is also known

that *BMP4* regulates cell proliferation and apoptosis in the brain and optic cup (Trousse et al., 2001).

We have created a functional dominant-negative ISWI mutant, which will be an excellent tool to dissect ISWI function, by interfering with ISWI function at specific times or in specific tissues during development. By placing DN-ISWI under control of neural-specific promoters, for example, we can test the role of ISWI in specific neural pathways in future studies.

This study has focused on the role of ISWI, which is involved in at least four different complexes in *Xenopus*. Ultimately, we intend to determine which of these ISWI complexes are responsible for the specific defects we observe by targeting subunits unique to each complex, using the methods described in this work. These future experiments will allow us to examine the specific interactions of chromatin remodelers and their targets during neural development in *Xenopus*.

4.1. Chromatin remodeling and neural development

Chromatin remodeling complexes are often thought of as ubiquitous factors that control the expression of large numbers of genes. It is therefore somewhat surprising to find that so many remodeling complexes appear to be specific for neural tissue, including *Xenopus*, human, murine and *Drosophila* ISWI homologs. In addition to the ISWI complexes, other SWI2/SNF2 family members appear to be critical in neural development. The human CHD5 remodeler is localized in neural tissue and is suspected to play a role in embryonic development (Thompson et al., 2003). BAF53b, part of the human SWI/SNF remodeling complex, is localized in postmitotic neurons and may create neuronal-specific patterns of chromatin accessibility (Olave et al., 2002). BAF57, a *Xenopus* SWI/SNF subunit, works in conjunction with Xsmad7 to increase expression of neural markers in *Xenopus* ectodermal explants (Domingos et al., 2002). Numerous SWI2/SNF2 family members exhibit neural expression patterns in *Xenopus* (Linder et al., 2004). Finally, the human SNF2L complex hNURF is enriched in the brain and regulates human *Engrailed*, a homeodomain protein that regulates neuronal development in the mid-hindbrain (Barak, 2003).

ISWI is turning out to be a surprisingly diverse subfamily of the SNF2 superfamily. *Drosophila* has three ISWI-containing complexes, yeast and *Xenopus* have four, and mammals appear to have seven distinct ISWI complexes. ISWI-containing complexes tend to have fewer subunits (2–4) relative to SNF2 subfamily containing complexes (~12). In biochemical assays, SNF2-subfamily complexes tend to disrupt nucleosome structure, while ISWI-subfamily complexes have been observed to enhance chromatin structure by equalizing nucleosome spacing, and to assemble nucleosomes (Lusser and Kadonaga, 2003). ISWI also has a unique requirement for histone tails for nucleosome remodeling (Clapier et al., 2002). Recently the

crystal structure of the nucleosome recognition module of ISWI was determined and an ISWI-specific DNA binding domain called SLIDE, in a region essential for H4 binding, was identified adjacent to the SANT domain (Grune et al., 2003). It is clear from many studies how important ISWI-containing complexes are to the development and/or function of each organism in which these complexes have been described. Each chromatin-remodeling complex, despite the similarities of their biochemical activities in vitro, may have far more specialized roles in gene expression and other cellular functions than previously suspected.

Acknowledgements

We wish to thank Dr Paul Wade (Emory University) for providing ISWI clones and antibodies, Dr Richard Harland (UC Berkeley) for GFP plasmids and advice, and Dr Tim Hinterberger (UA Anchorage) for advice and discussions. This work was funded by an Alaska EPSCoR grant (NSF EPS-0092040) to J.E.K and Alaska EPSCoR Graduate Research Fellowships to S.S.D, NIH/NEI grant EY09844 to J.J.H., and NIH/NEI grant EY016029-01 to J.E.K.

References

- Aihara, T., Miyoshi, Y., Koyama, K., Suzuki, M., Takahashi, E., Monden, M., Nakamura, Y., 1998. Cloning and Mapping of SMARCA5 encoding hSNF2H, a novel human homologue of Drosophila ISWI. *Cytogenet. Cell Genet.* 81, 191–193.
- Amaya, L., Taylor, D., Russell-Eggitt, I., Nischal, K.K., Lengyel, D., 2003. The morphology and natural history of childhood cataracts. *Surv. Ophthalmol.* 48 (2), 125–144.
- Audic, Y., Boyle, B., Slevin, M., Hartley, R.S., 2001. Cyclin E morpholino delays embryogenesis in *Xenopus*. *Genesis* 30 (3), 107–109.
- Badenhorst, P., Voas, M., Rebay, I., Wu, C., 2002. Biological functions of the ISWI chromatin remodeling complex NURF. *Genes Dev.* 16 (24), 3186–3198.
- Barak, O., Lazzaro, M.A., Lane, W.S., Speicher, D.W., Picketts, D.J., Shiekhattar, R., 2003. Isolation of human NURF: a regulator of Engrailed gene expression. *Embo. J.* 22 (22), 6089–6100.
- Bochar, D.A., Savard, J., Wang, W., Lafleur, D.W., Moore, P., Cote, J., Shiekhattar, R., 2000. A family of chromatin remodeling factors related to Williams syndrome transcription factor. *Proc. Natl. Acad. Sci. U S A.* 97, 1038–1043.
- Boerkoel, C.F., Takashima, H., John, J., Yan, J., Stankiewicz, P., Rosenbarker, L., Andre, J.L., B, A., Bogdanovic, R., Cockfield, S., Cordeiro, I., Frund, S., Illies, F., Joseph, M., Kaitila, I., Lama, L.C.G., McLeod, D.R., Milford, D.V., Petty, E.M., Rodrigo, F., Saraiva, J.M., Schmidt, B., Smith, G.C., S, A., Spranger, J., Thiele, H., Tizard, J., Weksberg, R., Lupski, J.R., Stockton, D.W., 2002. Mutant chromatin remodeling protein SMARCA1 causes Schimke immuno-osseousdysplasia. *Nat Genet.* 30, 215–220.
- Bozhenok, L., Wade, P.A., Varga-Weisz, P., 2002. WSTF-ISWI chromatin remodeling complex targets heterochromatic replication foci. *Embo. J.* 21 (9), 2231–2241.
- Citterio, E., Van Den Boom, V., Schnitzler, G., Kanaar, R., Bonte, E., Kingston, R.E., Hoeijmakers, J.H., Vermeulen, W., 2000. ATP-dependent chromatin remodeling by the Cockayne syndrome B DNA repair-transcription-coupling factor. *Mol. Cell Biol.* 20 (20), 7643–7653.
- Clapier, C.R., Nightingale, K.P., Becker, P.B., 2002. A critical epitope for substrate recognition by the nucleosome remodeling ATPase ISWI. *Nucleic. Acids Res.* 30 (3), 649–655.
- de la Serna, I.L., Carlson, K.A., Imbalzano, A.N., 2001. Mammalian SWI/SNF complexes promote MyoD-mediated muscle differentiation. *Nat. Genet.* 27 (2), 187–190.
- Demeret, C., Bocquet, S., Lemaitre, J.M., Francon, P., Mechali, M., 2002. Expression of ISWI and its binding to chromatin during the cell cycle and early development. *J. Struct. Biol.* 140 (1-3), 57–66.
- Deuring, R., Fanti, L., Armstrong, J.A., Sarte, M., Papoulas, O., Prestel, M., Daubresse, G., Verardo, M., Moseley, S.L., Berloco, M., Tsukiyama, T., Wu, C., Pimpinelli, S., Tamkun, J.W., 2000. The ISWI chromatin-remodeling protein is required for gene expression and the maintenance of higher order chromatin structure in vivo. *Mol. Cell* 5 (2), 355–365.
- Dirscherl, S.S., Krebs, J.E., 2004. Functional diversity of ISWI complexes. *Biochem. Cell Biol.* 82 (4), 482–489.
- Domingos, P.M., Obukhanych, T.V., Altmann, C.R., Hemmati-Brivanlou, A., 2002. Cloning and developmental expression of Baf57 in *Xenopus laevis*. *Mech. Dev.* 116 (1-2), 177–181.
- Doniach, T., 1993. Planar and vertical induction of anteroposterior pattern during the development of the amphibian central nervous system. *J. Neurobiol.* 24, 1256–1275.
- Eisen, J.A., Sweder, K.S., Hanawalt, P.C., 1995. Evolution of the SNF2 family of proteins: subfamilies with distinct sequences and functions. *Nucleic Acids Res.* 23 (4), 2715–2723.
- Furuta, Y., Hogan, B.L., 1998. BMP4 is essential for lens induction in the mouse embryo. *Genes Dev.* 12 (23), 3764–3775.
- Grune, T., Brzeski, J., Eberharter, A., Clapier, C.R., Corona, D.F., Becker, P.B., Muller, C.W., 2003. Crystal structure and functional analysis of a nucleosome recognition module of the remodeling factor ISWI. *Mol Cell.* 12, 449–460.
- Guschin, D., Geiman, T.M., Kikyo, N., Tremethick, D.J., Wolffe, A.P., Wade, P.A., 2000. Multiple ISWI ATPase complexes from *xenopus laevis*. Functional conservation of an ACF/CHRAC homolog. *J. Biol. Chem.* 275 (45), 35248–35255.
- Harland, R., Gerhart, J., 1997. Formation and function of Spemann's organizer. *Annu. Rev. Cell Dev. Biol.* 13, 611–667.
- Henry, J.J., Grainger, R.M., 1990. Early tissue interactions leading to embryonic lens formation in *Xenopus laevis*. *Dev. Biol.* 141 (1), 149–163.
- Humason, G.L., 1972. *Animal Tissue Techniques*. W.H. Freeman and Comp, San Francisco, CA.
- Khavari, P.A., Peterson, C.L., Tamkun, J.W., Mendel, D.B., Crabtree, G.R., 1993. BRG1 contains a conserved domain of the SWI2/SNF2 family necessary for normal mitotic growth and transcription. *Nature* 366, 170–174.
- Khokha, M.K., Yeh, J., Grammer, T.C., Harland, R.M., 2005. Depletion of three BMP antagonists from Spemann's organizer leads to a catastrophic loss of dorsal structures. *Dev. Cell* 8 (3), 401–411.
- Khorasanizadeh, S., 2004. The nucleosome. From genomic organization to genomic regulation. *Cell* 116 (2), 259–272.
- Knecht, A.K., Bronner-Fraser, M., 2002. Induction of the neural crest: A multigene process. *Nat. Rev. Genet.* 3 (6), 453–461.
- Krebs, J.E., Kuo, M.H., Allis, C.D., Peterson, C.L., 1999. Cell cycle-regulated histone acetylation required for expression of the yeast HO gene. *Genes Dev.* 13 (11), 1412–1421.
- Lazzaro, M.A., Picketts, D.J., 2001. Cloning and characterization of the murine Imitation Switch (ISWI) genes: differential expression patterns suggest distinct developmental roles for Snf2h and Snf2l. *J. Neurochem.* 77 (4), 1145–1156.
- Linder, B., Cabot, R.A., Schwickert, T., Rupp, R.A., 2004. The SNF2 domain protein family in higher vertebrates displays dynamic expression patterns in *Xenopus laevis* embryos. *Gene* 326, 59–66.

- Lusser, A., Kadonaga, J.T., 2003. Chromatin remodeling by ATP-dependent molecular machines. *Bio Essays* 25, 1192–1200.
- Maeda, R., Mood, K., Jones, T.L., Aruga, J., Buchberg, A.M., Daar, I.O., 2001. Xmeis1, a protooncogene involved in specifying neural crest cell fate in *Xenopus* embryos. *Oncogene* 20, 1329–1342.
- Marti, E., Bovolenta, P., 2002. Sonic hedgehog in CNS development: one signal, multiple outputs. *Trends Neurosci.* 25 (2), 89–96.
- Mathis, L., Nicolas, J.F., 2002. Cellular patterning of the vertebrate embryo. *Trends Genet.* 18, 627–635.
- Merzdorf, C.S., Goodenough, D.A., 1997. Localization of a novel 210 kDa protein in *Xenopus* tight junctions. *J. Cell. Sci.* 110, 1005–1012.
- Nieuwkoop, P.D., 1999. The neural induction process; its morphogenetic aspects. *Int. J. Dev. Biol.* 43 (7), 615–623.
- Nieuwkoop, P.D., Faber, J., 1967. *Normal Table of Xenopus Laevis*. Daudine, North-Holland, Amsterdam.
- Okabe, I., Bailey, L.C., Attree, O., Srinivasan, S., Perkel, J.M., Laurent, B.C., Carlson, M., Nelson, D.L., Nussbaum, R.L., 1992. Cloning of human and bovine homologs of SNF2/SWI2: a global activator of transcription in yeast *S. cerevisiae*. *Nucleic. Acids Res.* 20 (17), 4649–4655.
- Olave, I., Wang, W., Xue, Y., Kuo, A., Crabtree, G.R., 2002. Identification of a polymorphic, neuron-specific chromatin remodeling complex. *Genes Dev.* 16 (19), 2509–2517.
- Picketts, D.J., Higgs, D.R., Bachoo, S., Blake, D.J., Quarrell, O.W., Gibbons, R.J., 1996. ATRX encodes a novel member of the SNF2 family of proteins: Mutations point to a common mechanism underlying the ATR-X syndrome. *Hum. Mol. Genet.* 5, 1899–1907.
- Richmond, E., Peterson, C.L., 1996. Functional analysis of the DNA-stimulated ATPase domain of yeast SWI2/SNF2. *Nucleic Acids Res.* 24 (19), 3685–3692.
- Sambrook, J., Fritsch, E.F., Maniatis, T., 1989. *Molecular Cloning*. Habor Laboratory Press, New York, Cold Springs.
- Sive, H.L., Grainger, R.M., Harland, R.M., 2000. *Early Development of Xenopus Laevis*. Cold Spring Harbor Laboratory Press, New York.
- Thompson, P.M., Gotoh, T., Kok, M., White, P.S., Brodeur, G.M., 2003. CHD5, a new member of the chromodomain gene family, is preferentially expressed in the nervous system. *Oncogene* 22, 1002–1011.
- Trousse, F., Esteve, P., Bovolenta, P., 2001. Bmp4 mediates apoptotic cell death in the developing chick eye. *J. Neurosci.* 21 (4), 1292–1301.
- Weinstein, D.C., Hemmati-Brivanlou, A., 1999. Neural induction. *Annu. Rev. Cell Dev. Biol.* 15, 411–433.
- Zuber, M.E., Gestri, G., Viczian, A.S., Barasacchi, G., Harris, W.A., 2003. Specification of the vertebrate eye by a network of eye field transcription factors. *Development* 130, 5155–5167.